Neotropical Ichthyology

Original article

https://doi.org/10.1590/1982-0224-2022-0075

urn:lsid:zoobank.org:pub:4FD4576C-30E9-49A0-B668-9D2C01BE312A

New species of *Rhyacoglanis* (Siluriformes: Pseudopimelodidae) from the upper rio Tocantins basin

Correspondence:
Oscar Akio Shibatta
shibatta@uel.br

Oscar Akio Shibatta and Lenice Souza-Shibatta

A new species of *Rhyacoglanis* from the upper rio Tocantins basin is described based on morphological and molecular data. The new species differs from the congeners by its color pattern, caudal fin shape, hypural bones fusion pattern, pectoral-fin spine shape, and barcode sequence of cytochrome oxidase subunit I (COI). In this study, two putative monophyletic groups of *Rhyacoglanis* are proposed based on morphology, one consisting of species with a short post-cleithral process and caudal fin with rounded lobes, *Rhyacoglanis epiblepsis* and *R. rapppydanielae*, and the other with a longer post-cleithral process and caudal fin with pointed lobes, *R. annulatus*, *R. paranensis*, *R. pulcher*, *R. seminiger*, and the new species described herein.

Keywords: Biodiversity, Bumblebee catfish, Ostariophysi, Systematics, Taxonomy.

Submitted July 27, 2022
Accepted December 7, 2022
by Carlos DoNascimiento
Epub February 20, 2023

Online version ISSN 1982-0224
Print version ISSN 1679-6225

Neotrop. Ichthyol.
vol. 21, no. 1, Maringá 2023

Museu de Zoologia, Departamento de Biologia Animal e Vegetal, Centro de Ciências Biológicas, Universidade Estadual de Londrina, Rodovia Celso Garcia Cid, km 380, 86051-970 Londrina, PR, Brazil. (OAS) shibatta@uel.br (corresponding author), (LSS) lenicesouza@hotmail.com.

Uma nova espécie de *Rhyacoglanis* da bacia do alto rio Tocantins é descrita com base em dados morfológicos e moleculares. A nova espécie difere das congêneres por seu padrão de colorido, forma da nadadeira caudal, padrão de fusão dos ossos hipurais, forma do espinho da nadadeira peitoral e sequência de código de barras do citocromo oxidase subunidade I (COI). Neste estudo, dois possíveis grupos monofiléticos de *Rhyacoglanis* são propostos com base na morfologia, constituídos por espécies com o processo pós-cleithral curto e nadadeira caudal com lóbulos arredondados, *Rhyacoglanis epiblepsis* e *R. rapppydanielae*, e o outro com o processo pós-cleithral mais alongado e nadadeira caudal com lóbulos pontiagudos, *R. annulatus*, *R. paranensis*, *R. pulcher*, *R. seminiger*, e a nova espécie aqui descrita.

Palavras-chave: Bagrinho, Biodiversidade, Ostariophysi, Sistemática, Taxonomia.

INTRODUCTION

Pseudopimelodidae Fernández-Yépez & Antón, 1966 is a small family of Neotropical catfishes with 54 known species (Shibatta *et al*., 2021a,b). It comprises six genera, distributed in the subfamilies Pseudopimelodinae (*Cruciglanis* Ortega-Lara & Lehmann, 2006, *Pseudopimelodus* Bleeker, 1858, and *Rhyacoglanis* Shibatta & Vari, 2017) and Batrocoglaninae (*Batrochoglanis* Gill, 1858, *Lophiosilurus* Steindachner, 1876, and *Microglanis* Eigenmann, 1912) (Shibatta *et al*., 2021; Silva *et al*., 2021).

Rhyacoglanis comprises six species: *R. annulatus* Shibatta & Vari, 2017; *R. epiblepsis* Shibatta & Vari, 2017; *R. paranensis* Shibatta & Vari, 2017; *R. pulcher* (Boulenger, 1887); *R. rapppydanielae* Shibatta, Rocha & Oliveira, 2021, and *R. seminiger* Shibatta & Vari, 2017. The genus can be identified by the following morphological characters: small size (maximum known size of 89.2 mm standard length – SL), premaxillary dentigerous plate posterolaterally pointed, lateral line elongated, lateral region of the head with rounded shape depigmented area, body with dark brown vertical bars, and caudal fin with dark brown band usually confluent midlaterally with the dark brown bar on the caudal peduncle (Shibatta, Vari, 2017). The monophyly of *Rhyacoglanis* is corroborated by morphological and molecular analyses (Shibatta, Vari, 2017; Shibatta *et al*., 2021; Silva *et al*., 2021).

Rhyacoglanis is distributed in the Amazon, Orinoco, Paraná, Paraguay, and lower rio Tocantins basins (Shibatta, Vari, 2017; Shibatta *et al*., 2021). *Microglanis maculatus* Shibatta, 2014 is the only species of Pseudopimelodidae described from the upper rio Tocantins basin. This region is considered highly endemic and has 27 (52.9%) of the 51 threatened fish species in the entire rio Tocantins-Araguaia basin (Chamon *et al*., 2022). The new species of *Rhyacoglanis* described herein reinforces the endemicity of fishes in the basin.

MATERIAL AND METHODS

Measurements and counts were made according to Shibatta, Vari (2017). Comparative material is listed in Shibatta, Vari (2017) and Shibatta *et al*. (2021b), except as mentioned in this contribution. Osteological and lateral line nomenclature followed Shibatta (2019). The brain of a specimen of the new species was presented in Abrahão *et al*. (2018). A principal component analysis (PCA) was performed with the aid of the program Past (Hammer *et al*., 2001) using the covariance matrix of the log data. The analysis compared the new species to *R. rapppydanielae,* the only congener from the rio Tocantins basin, and *R. paranensis*, the closest species with respect to morphology and geography. Specimens were cleared and stained (C&S) following Dingerkus, Uhler (1977). The counts were made on C&S specimens (n = 5), X-rayed specimens (x-r; n = 2), and ethanol-preserved specimens (eth; n = 11). Counts are presented as frequencies throughout the description, and those for the holotype are highlighted with an asterisk.

The distribution map was constructed with Quantum GIS software v.1.7.0 (QGIS Development Team, 2011) with a 'kml' file obtained with the help of Google Earth Pro (2021). Samples from the following collections were examined: Laboratório de Biologia e Genética de Peixes, Universidade Estadual Paulista "Júlio Mesquita Filho", São Paulo (LBP), Museu de Ciências e Tecnologia da Pontifícia Universidade Católica do Rio Grande do Sul, Porto Alegre (PUCRS), Museu de Zoologia da Universidade Estadual de Londrina, Londrina (MZUEL), and Museu de Zoologia da Universidade de São Paulo, São Paulo (MZUSP).

Genomic DNA was extracted from muscle tissues using an extraction kit (Wizard Genomic DNA Purification – PROMEGA), following the manufacturer's protocol. A segment of approximately 648 bp from the 5' end of the mitochondrial cytochrome c oxidase subunit I (COI) gene was amplified by polymerase chain reaction (PCR) using primers FishF1 and FishR1 (Ward *et al*., 2005), following the PCR conditions proposed by Hajibabaei *et al*. (2005). PCR products were visualized on a 0.8% agarose gel, stained with SYBR® Safe DNA Gel Stain (Life Technologies), following the manufacturer's protocol, and purified using ExoSAP IT® (Prodimol Biotecnologia). The samples were then sequenced, and the product of the sequencing reactions was analyzed in an ABI 3500 XL automatic sequencer (Applied Biosystems Inc., CA, USA) using ABI Big Dye Terminator v 3.1. The sequences were aligned and edited in the MEGA v.6 software (Tamura *et al*., 2013), together with other sequences of pseudopimelodids retrieved from GenBank (https://www.ncbi.nlm.nih.gov/genbank/) or the BOLD Systems databases (https://www.boldsystems.org/). The sequences generated in the study were deposited in GenBank under accession numbers OP062253 to OP062256. Intraspecific and interspecific genetic distances were calculated using the Kimura-two-parameter model (Kimura, 1980) with Mega v.6. Four species delimitation methods were used to test the hypothesis of new species: Automatic Barcode Gap Discovery – ABGD (Puillandre *et al*., 2012), Assemble Species by Automatic Partitioning – ASAP (Puillandre *et al*., 2021), Bayesian Poisson Tree Process – bPTP (Zhang *et al*., 2013), and Generalized Mixed Yule-Coalescent – GMYC (Pons *et al*., 2006). For bPTP, a maximum likelihood tree was generated in Mega v.6, and the analysis was performed through the website https://species.h-its.org/ptp/. A file with the aligned sequences was used on the online servers for ABDG and ASAP (https://bioinfo.mnhn.fr/abi/public/abgd/abgdweb.html

and https://bioinfo.mnhn.fr/abi/public/asap/asapweb.html). The GMYC method was performed in the Splits package (Pons *et al*., 2006; Fujisawa, Barraclough, 2013) using an ultrametric tree with the R 3.5.1 program. The ultrametric tree was obtained via Bayesian inference in the program BEAST v. 2.6.2 (Bouckaert *et al*., 2019) with a strict molecular clock and a birth-death model (Heled, Drummond, 2010). The data were analyzed as a single partition, and the evolutionary model used was HKY+G, previously specified by the jModelTest2 (Darriba *et al*., 2012). The analyses were carried out for 100 million generations, sampling a tree every 1000 generations. TRACER v.1.5 (BEAST package) was used to verify the subsequent probability of sufficient minimum effective size (ESS> 200) and a significant estimate of the parameters and the average age of the nodes, considering a burn-in of 25 million generations. The trees were summarized and visualized using TREEANNOTATOR 1.5.3 and FIGTREE 1.3.1, respectively (Drummond, Rambaut, 2007; Rambaut, 2009).

RESULTS

Rhyacoglanis varii, new species

urn:lsid:zoobank.org:act:2A1AD513-0AB2-4D10-91AA-9C3F865A7152

(Figs. 1–3; Tab. 1)

Rhyacoglanis sp. —Abrahão *et al*., 2018:3 [brain gross morphology].

Holotype. MZUEL 22317, 67.1 mm SL, Brazil, Goiás, upper rio Tocantins basin, rio do Peixe, Goianésia, 15°28'23.8"S 49°13'28.9"W, 14 Jul 2010, O. A. Shibatta, E. Santana, A. Claro-García & L. R. Jarduli.

Paratypes (20 specimens). MZUEL 6039, 29.6–69.1 (10 eth, 5 C&S; 4 COI), 25.6–69.1 mm SL, same data as the holotype. MZUSP 54082, 5 eth, 37.0–47.6 mm SL, Brazil, Goiás, rio Tocantinzinho and tributaries, Serra da Mesa region, Minaçu, 14°12'32.02"S 48°04'15.17"W, 28 Oct to 4 Nov 1996, MZUSP/MNRJ staff.

Diagnosis. *Rhyacoglanis varii* is easily distinguished from congeners (except for *R. pulcher*) by the color pattern, with the dark brown vertical bar below the dorsal-fin base not confluent with a dark brown bar below the adipose-fin base (*vs*. broadly confluent in *R. seminiger*), the subdorsal dark brown bar becomes abruptly thinner ventrally (*vs*. broader in *R. paranensis*), dark brown spots sparsely distributed on the body (*vs*. dense in *R. epiblepsis* and *R. rapppydanielae*), and a solid dark brown bar on caudal peduncle (*vs*. becoming light brown inside, resembling a circle, in *R. annulatus*). *Rhyacoglanis varii* has the posterior tip of the post-cleithral process reaching vertical through the base of the dorsal-fin spine (*vs*. not reaching in *R. epiblepsis* and *R. rappydanielae*). *Rhyacoglanis varii* differs from *R. paranensis* by the longer distance of anus to anal-fin origin (mean = 11.4±0.8% *vs*. 10.0±1.4% SL), maxillary barbel length (mean = 79.6±5.8% *vs*. 74.8±8.7% SL), and caudal peduncle depth (mean = 9.5±0.5% *vs*. 8.8±0.5% SL); minor posterior

nostril to eye distance (mean = 4.8±0.9% *vs*. 6.7±1.3% SL), body depth (mean = 18.2±1.5% *vs*. 21.4±2.6% SL), and postcleithral process length (mean = 12.9±1.1% *vs*. 13.9±1.2% SL). *Rhyacoglanis varii* differs from *R. pulcher* and *R. seminiger* by the shape of the pectoral-fin spine, with anterior serrae distributed along the entire margin (*vs*. restricted to the proximal half).

FIGURE 1 | Holotype of *Rhyacoglanis varii*, MZUEL 22317, 67.1 mm SL, rio do Peixe, upper rio Tocantins basin, Goianésia, state of Goiás, Brazil.

Description. Body proportions are given in Tab. 1. Body depressed from snout tip to dorsal-fin origin; progressively compressed from that point to caudal-fin base. Dorsal profile of head and anterior body scarcely convex from snout tip to dorsal-fin origin, then nearly straight, scarcely descending to adipose-fin origin. Ventral head convex, then almost straight from pectoral-fin origin to posterior limit of anal-fin base. Caudal peduncle profile slightly concave along dorsal and ventral margins. Head depressed; slightly longer than wide; anterior margin convex (semicircular) in dorsal view. Head with weakly developed unculiferous tubercles scattered laterally and dorsally. Mouth terminal and wide; width more than one-half of head length (HL). Upper jaw slightly longer than, or same length as, lower jaw. Lips thick and well developed, more so proximate to rictus. Premaxillary tooth plate posterolaterally pointed. Anterior nostril immediately posterior to vertical through rictus. Eye small, superior, covered by skin, slightly posterior to anterior one-third of HL. Opercular membrane well developed; margin falling short of pectoral-fin origin. Maxillary barbel base enlarged. Tip of adpressed maxillary barbel falling short of opercular margin. Adpressed inner mental barbel tip surpassing outer mental barbel base but falling short of its tip. Adpressed outer mental barbel tip reaching opercular membrane margin. Dorsal-fin trapezoidal, distal margin rounded, and first branched ray longer than dorsal-fin base. Dorsal-fin origin immediately posterior to anterior one-third of body but anterior to one-half of SL. Adpressed dorsal-fin tip reaching slightly beyond midpoint between dorsal-fin base terminus and adipose-fin origin. First dorsal-fin ray (spinelet) small, rigid, forming dorsal-fin spine-locking mechanism. Second dorsal-fin ray forming strong, rigid, pointed spine; anterior margin smooth, posterior margin with retrorse serrations. Dorsal-fin rays II,6* (5 C&S, 16 eth). Adipose fin long; base longer than anal-fin base; posterior margin free and rounded. Pectoral-fin margin somewhat triangular, posterior margin rounded. Adpressed pectoral fin tip falling short pelvic-fin origin. First pectoral-fin ray forming strong, rigid, pointed spine, serrated along anterior and posterior margins; posterior serrae retrorse, distinctly larger than anterior serrae (approximately twice as long); pectoral-fin spine notched distally (Fig. 2). Pectoral-fin rays I,6* (5 C&S, 15 eth), I,5 (1 eth). Pelvic-fin profile almost triangular; posterior margin rounded. Pelvic-fin origin immediately posterior to vertical through dorsal-fin base terminus. Adpressed pelvic fin tip reaching vertical through adipose fin origin. Pelvic-fin rays i,5* (5 C&S, 16

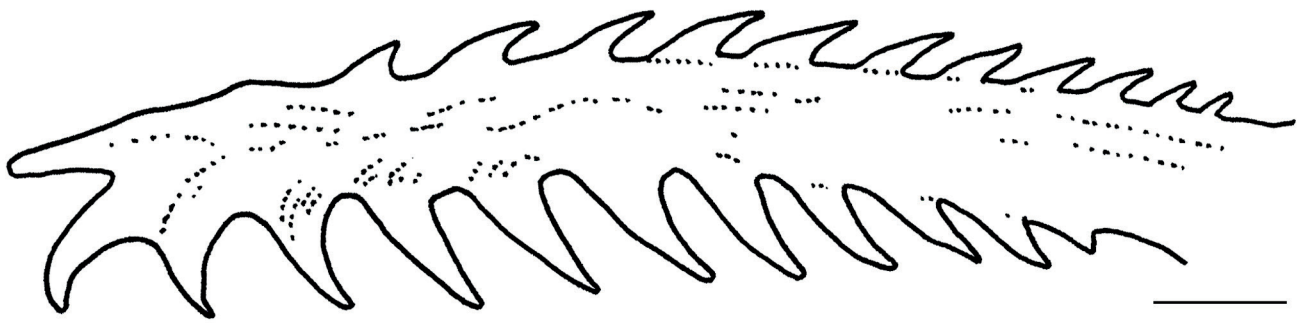

FIGURE 2 | *Rhyacoglanis varii* pectoral-fin spine, paratype, MZUEL 6039, 55.5 mm SL. Scale bar = 1.0 mm.

eth). Anal-fin margin rounded; anal-fin rays iii,5 (1 eth), ii,6* (5 eth), iii,6 (9 eth), iv,6 (1 C&S, 1 eth), v,5 (1 C&S), or v,6 (3 C&S). Caudal fin forked; lobes pointed; ventral lobe usually slightly longer than dorsal lobe. Caudal-fin principal rays i,6,5,i (1 eth), i,6,7,i (1 C&S, 1 eth), i,6,8,i* (4 C&S, 13 eth) or i,7,8,i (1 eth). Dorsal procurrent rays 17 (1 C&S), 18 (1 C&S), or 19 (3 C&S); ventral procurrent rays 15 (3 C&S), 16 (1 C&S), or 17 (1 C&S). Skeletal elements supporting the caudal fin as follow: parhypural, hypurals 1 and 2 fused; hypural 3 and 4 fused; hypural 5 free (Fig. 3). Posterior cleithral process well developed, pointed, tip reaching vertical through anterior dorsal-fin base. Axillary pore present. Lateral line complete. Total vertebrae 33 (2 x-r), 35 (3 C&S), 36 (2 C&S). Ribs 8 (1 X-r), 9 (3 C&S, 1 X-r), 10 (1 C&S), or 11 (1 C&S). Gill rakers 1,0,5* (1 C&S, 5 eth), 1,0,6 (2 C&S, 2 eth), 1,0,7 (6 eth), 1,0,8 (2 eth), 1,1,5 (2 C&S). Branchiostegal rays 7 (1 C&S), 8 (4 C&S).

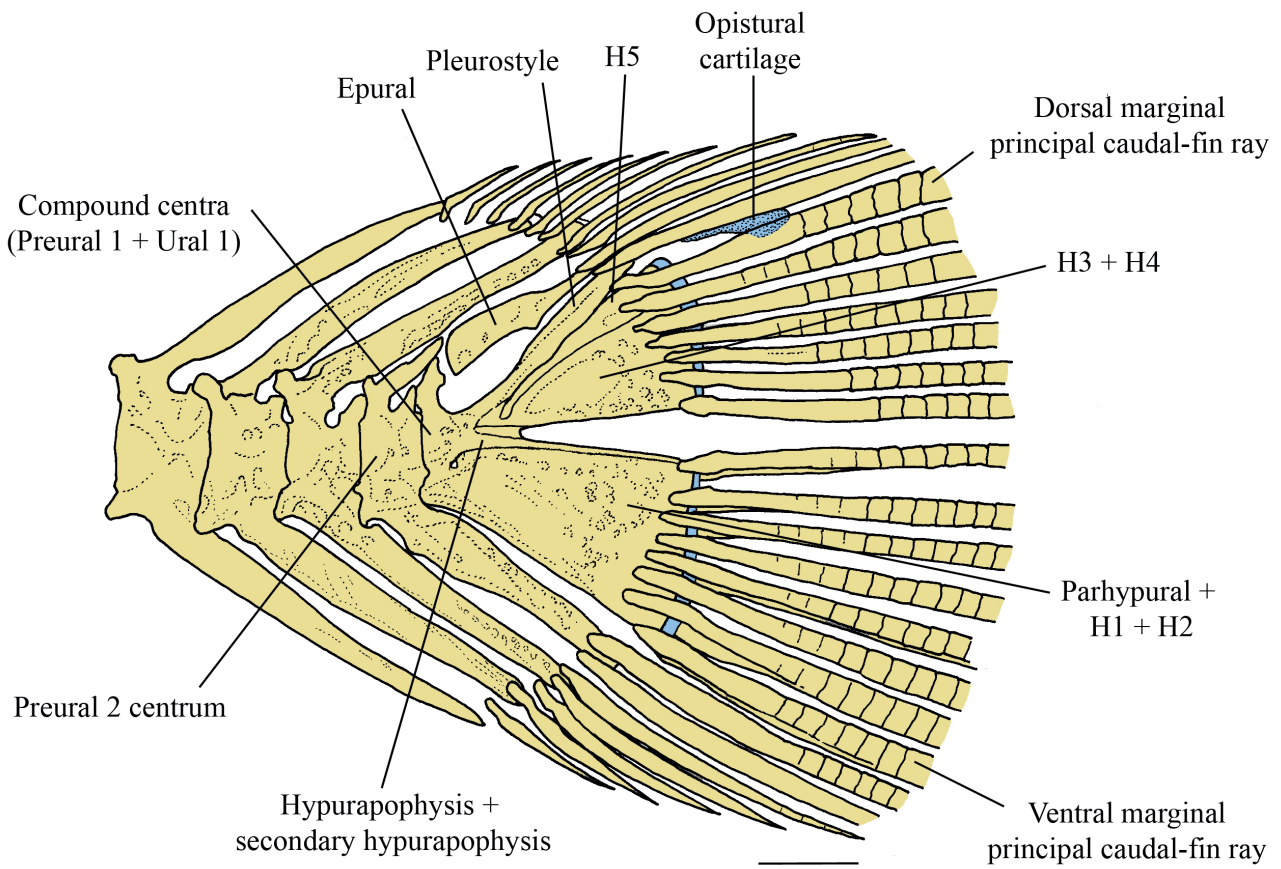

FIGURE 3 | *Rhyacoglanis varii* caudal-fin skeleton, paratype, MZUEL 6039, 53.5 mm SL. Bones in yellow ocher and cartilage in blue. H1 to H5 = hypurals 1 to 5. Scale bar = 1.0 mm.

TABLE 1 | Morphometry of *Rhyacoglanis varii* from upper rio Tocantins basin (n = 42). Statistics of minimum (Min), maximum (Max), mean, and standard deviation (SD) include holotype.

	Holotype	Min-Max	Mean±SD
Standard length (mm)	67.1	29.6–69.1	44.3±11.1
Percent of standard length			
Head length	30.6	27.0–30.6	28.8±1.0
Pectoral girdle width	27.6	23.1–28.4	26.5±1.3
Predorsal distance	37.3	35.1–37.5	36.4±0.8
Dorsal-fin base length	17.2	15.0–17.2	16.3±0.6
Adipose-fin base length	18.4	16.2–21.5	18.3±1.5
Prepelvic length	50.5	46.8–51.7	49.5±1.6
Pelvic fin to anal fin distance	24.7	22.5–25.7	24.1±0.9
Anal-fin base length	10.3	9.2–13.1	10.5±0.9
Caudal peduncle length	15.1	15.1–19.9	17.7±1.3
Body depth	20.7	16.1–21.2	18.2±1.5
Caudal peduncle depth	9.4	8.5–10.5	9.5±0.5
Pectoral-fin spine length	17.5	16.3–21.5	18.6±1.5
Dorsal-fin spine length	15.3	14.1–19.7	17.7±1.6
Pelvic fin length	19.6	17.4–19.8	18.8±0.7
Postcleithral process length	12.6	10.1–14.7	12.9±1.1
Dorsal fin to pelvic fin distance	26.2	22.4–26.2	23.8±1.2
Pelvic fins distance	13.7	10.9–13.7	12.3±0.7
Pelvic fin to anus distance	14.5	11.9–14.5	13.1±0.8
Anus to anal fin distance	11.9	9.8–12.5	11.4±0.8
Percentages of head length			
Eye diameter	9.4	8.9–11.8	10.4±0.8
Interorbital distance	31.1	26.3–34.5	31.7±1.9
Snout length	39.5	34.2–39.8	37.0±1.6
Mouth width	57.5	45.9–60.2	52.5±4.8
Head depth	39.4	35.0–50.9	41.0±4.5
Maxillary barbel length	75.7	72.0–92.9	79.6±5.8
Anterior to posterior nostrils distance	14.3	14.3–19.8	17.0±1.6
Posterior nostril to eye distance	5.5	3.4–6.2	4.8±0.9
Posterior nostrils distance	20.9	18.7–23.6	20.4±1.2

Head laterosensory canal and pores. Supraorbital(s) canal begins anteromedially to anterior nostril just before vertical through nostril, with five branches (s1, s2, s3, s6 (epiphyseal branch), and s8 (parietal branch)). Infraorbital canal with six branches (i1 to i6), bifurcated anteriorly; i1 lateral to anterior nostril; i2 between anterior and posterior nostrils (Fig. 4). Preoperculomandibular (pm) canal with ten branches; arched in ventral view; pm1 medio-ventral on head; pm9 at base of opercular bone; canal continuing dorsally, finishing with pm11 fused with first postotic branch (po1). Postotic canal with two branches (po1 and po2), followed posteriorly by trunk lateral-line canal.

Coloration in alcohol. Lateral surfaces of body with yellowish brown ground color. Dorsal surface of head light gray with scattered dark brown specks; pale yellow blotch on adductor muscle region. Maxillary barbel light brown with dark brown specks; mentonian barbel light yellow. Trunk and caudal regions with three dark brown bars. Subdorsal trunk bar approximately triangular, attenuated ventrally, lowermost portion slightly entering belly. Subadipose bar broad, spanning distance between bases of adipose and anal fins, and confluent with contralateral bar, shape roughly rectangular with anterior and posterior margins irregularly concave; rarely in extreme dorsal and ventral contact with dark brown bar on caudal peduncle. Caudal peduncle bar slightly narrower, approximately rectangular, anterior, and posterior margins irregularly concave, dorsally, and ventrally confluent with contralateral bar. Dark brown spots scattered throughout lateral region of body. Ventral region predominantly light yellow, without dark spots. Area between pelvic fins sometimes with tiny spots. Dorsal fin dark brown, distal third with hyaline band; occasionally, band of hyaline elliptical spots on membranes between rays in second lower quarter. Adipose fin with central dark brown vertical band completely separating light yellow spots on anterior and posterior regions, respectively. Pectoral fin hyaline with narrow dark brown band on median region.

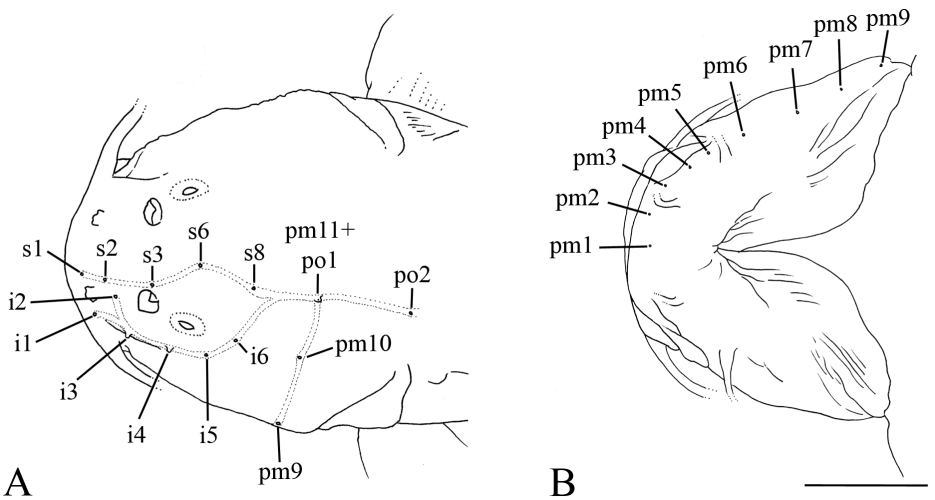

FIGURE 4 | *Rhyacoglanis varii* laterosensory canal pores, MZUSP 54082, 47.6 mm SL, paratype, in dorsal (**A**) and ventral views (**B**). i1 to i6 = infraorbital pores 1 to 6; pm1 to pm11 = preoperculomandubular pores 1 to 11; po1 and po2 = postotic pores 1 and 2; s1 to s8 = supraorbital pores 1 to 8. Scale bar = 5 mm.

Pelvic fin hyaline with irregular or inconspicuous dark brown band across middle of rays. Anal fin hyaline; dark brown, approximately triangular spot near origin, confluent with subadipose band; dark brown oval spots forming irregular band across middle rays. Caudal fin with 3-shaped dark brown band through posterior region; median tip usually confluent with the dark brown bar on caudal peduncle; distal margin hyaline (Fig. 1).

Coloration in life. Head dorsal region reddish-brown, lateral region with yellowish-brown spot, peppered with dark brown spots of about pupil size. Maxillary barbel base light-brown, grayish posteriorly. Eye gray. Trunk and caudal peduncle ground color light yellowish-brown, with three large black vertical bars (subdorsal, subadipose, and caudal peduncle), peppered with dark brown spots of eye diameter size. Subdorsal bar triangular; attenuated ventrally; subadipose bar trapezoidal; caudal peduncle bar vertically rectangular. Pectoral fin hyaline, reddish-brown, with dark brown band crossing middle of rays. Dorsal fin about 3/4 black, with distinct reddish-brown distal margin. Pelvic fin hyaline, reddish-brown, with dark brown spots crossing middle of rays. Adipose fin black with light brown spots on anterior and posterior regions, respectively. Anal fin light brown with dark brown band across middle of rays. Caudal fin hyaline, light brown, with 3-shaped black band on posterior half; distal margin hyaline (Fig. 5)

FIGURE 5 | *Rhyacoglanis varii* coloration in life, MZUEL 6039, paratype, 46.1 mm SL, rio do Peixe, upper rio Tocantins basin, Goianésia, state of Goiás, Brazil.

Geographical distribution. *Rhyacoglanis varii* is known only from the upper rio Tocantins basin on the Brazilian shield (Fig. 6).

Ecological notes. The type locality in the rio do Peixe presented clear running waters, mostly shallow, with deeper pools approximately knee height. The bottom is predominantly pebbles, with rocks, sand, and organic litter (Figs. 7A,B). The color pattern of the species, yellowish or orange-brown background with alternating dark brown bars, allows for perfect camouflage amid the rocks and litter (Fig. 7C). The area is in a rural and pristine zone, with marginal vegetation well preserved, which is the source of the organic litter. Dissolved oxygen 8.3 $mg.L^{-1}$, pH 8.06, conductivity 83.4µS. cm^{-1}, and temperature 22.5° C (at 12:54h Brasília time). Specimens were found under rocks, protected from the water current (Fig. 7C), and collected with a sieve with a high-density polyethylene mesh of 2 mm size as rocks were turned. The use of trawls or fishing nets was inefficient for their capture.

Etymology. The species name *varii* honors the ichthyologist Richard P. Vari (1949–2016) for his outstanding contributions to the systematics of Neotropical fishes.

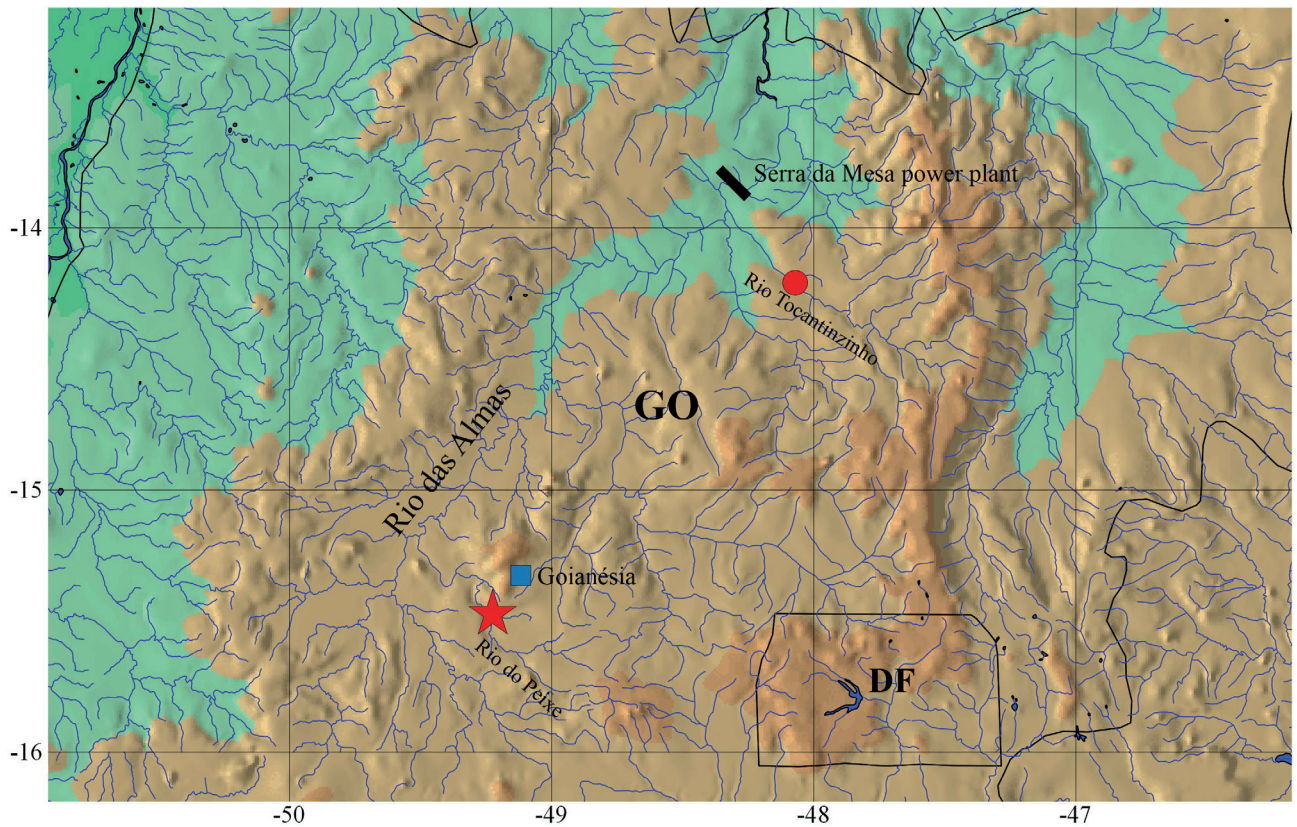

FIGURE 6 | Map of *Rhyacoglanis varii* distribution through upper rio Tocantins basin (red dot = rio Tocantinzinho tributary; red star = type locality, rio do Peixe), state of Goiás (GO), Brazil. DF = Federal District of Brazil.

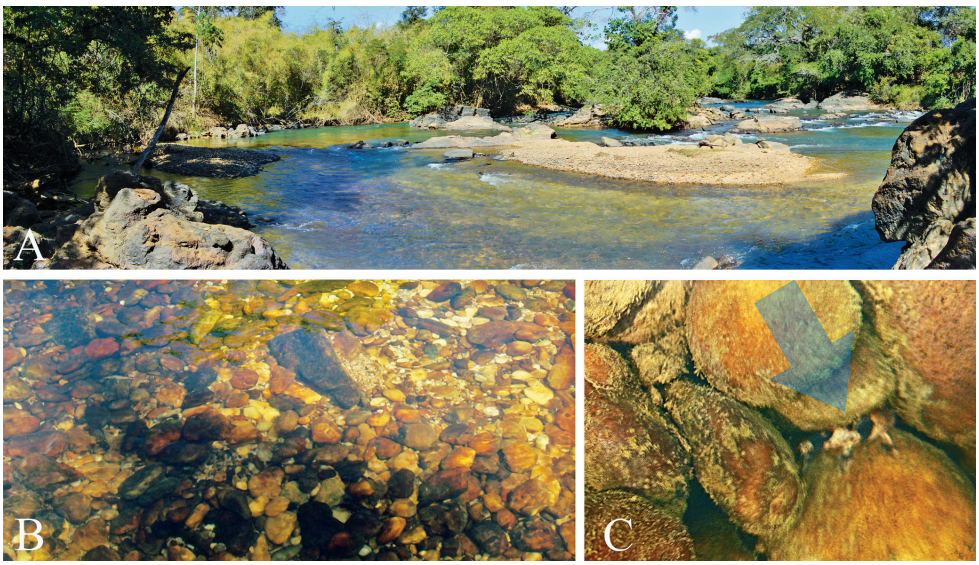

FIGURE 7 | **A.** Panoramic view of *Rhyacoglanis varii* type locality, rio do Peixe, Goianésia, state of Goiás, Brazil; **B.** Bottom with rocks, pebbles, and sand where specimens were collected; **C.** Blue arrow indicating water flow and pointing to a specimen beneath rocks.

Conservation status. Considering the criterion established by the IUCN Standards and Petitions Committee (IUCN, 2022), the species is Data Deficient (DD) because "very little information is known about a taxon, but the available information indicates that the taxon may be threatened". The species is apparently restricted to the upper Tocantins basin, but the absence of the species in several collections points out its low occurrence in the basin. For instance, in the same expedition when the species was collected, the effort failed to capture it in 18 other localities of Barro Alto, Goianésia, and Pirenópolis municipalities (OAS, pers. obs.). Furthermore, it is worth mentioning that the rapids environment where the species occurs often lends itself to the construction of hydroelectric plants. Dams entirely alter the river's flow and seasonality (Winemiller *et al*., 2016) and can thereby jeopardize the local population. Also, the dam of the Serra da Mesa power plant may obstruct movement between populations upstream and downstream of the dam.

Multivariate morphometric analysis. Differences in the shape of *Rhyacoglanis varii*, *R. paranensis*, and *R. rapppydanielae* are represented by the second and third axes of the principal components analysis (Fig. 8). The character loadings, eigenvalues, and percentage of variation are presented in Tab. 2. *Rhyacoglanis varii* differs from *R. paranensis* by the longer anus-to-anal-fin origin distance, maxillary barbel length, caudal peduncle depth (positive loadings), and minor posterior nostril-to-eye distance, body depth, and postcleithral process length (negative loadings). *Rhyacoglanis rapppydanielae* differs from *R. varii* and *R. paranensis* by the longer distance between posterior nostril to eye distance, anus to anal-fin origin distance, and mouth width (positive loadings), and by the smaller dorsal-fin spine length and post-cleithral process length (negative loadings).

TABLE 2 | Character loadings of the first three principal components axes of combined analysis of *Rhyacoglanis varii* (N = 16), *R. paranensis* (N = 31), and *R. rapppydanielae* (N = 13).

Characters	PC 1	PC 2	PC 3
Head length	0.1915	0.015	0.05995
Eye diameter	0.1345	0.09743	0.1875
Interorbital distance	0.1988	0.01607	-0.04845
Snout length	0.1942	-0.009734	0.02416
Mouth width	0.2077	0.1981	0.1694
Pectoral girdle width	0.2087	0.05512	0.01591
Predorsal distance	0.1722	0.01745	0.03117
Dorsal-fin base length	0.2031	-0.08244	-0.06269
Adipose-fin base length	0.1661	0.06053	0.1708
Prepelvic distance	0.186	0.02634	0.01305
Pelvic fin to anal fin distance	0.1913	0.1087	0.1432
Anal-fin base length	0.1823	-0.07779	0.001686
Caudal peduncle length	0.1888	-0.1205	0.1033
Head depth	0.2193	-0.09948	-0.003842
Body depth	0.2262	0.0633	-0.2802
Caudal peduncle depth	0.1791	0.09839	0.2062
Pectoral-fin spine length	0.1622	-0.1404	0.04719
Dorsal-fin spine length	0.171	-0.4545	-0.0166
Maxillary barbel length	0.1625	-0.03909	0.2676
Pelvic length	0.179	-0.1042	-0.05121
Anterior to posterior nostril distance	0.1462	0.05437	0.006021
Posterior nostril to eye distance	0.1529	0.5834	-0.5648
Posterior nostrils distance	0.2059	-0.04857	-0.002237
Postcleithral process length	0.2379	-0.4045	-0.273
Dorsal fin to pelvic fin distance	0.215	0.09364	-0.02694
Pelvic fin distance	0.1971	0.08527	-0.1839
Pelvic fin to anus distance	0.2148	-0.08011	-0.1393
Anus to anal fin distance	0.1499	0.3313	0.4677
Eigenvalue	0.333129	0.0280641	0.0112928
% variance	83.209	7.0099	2.8207

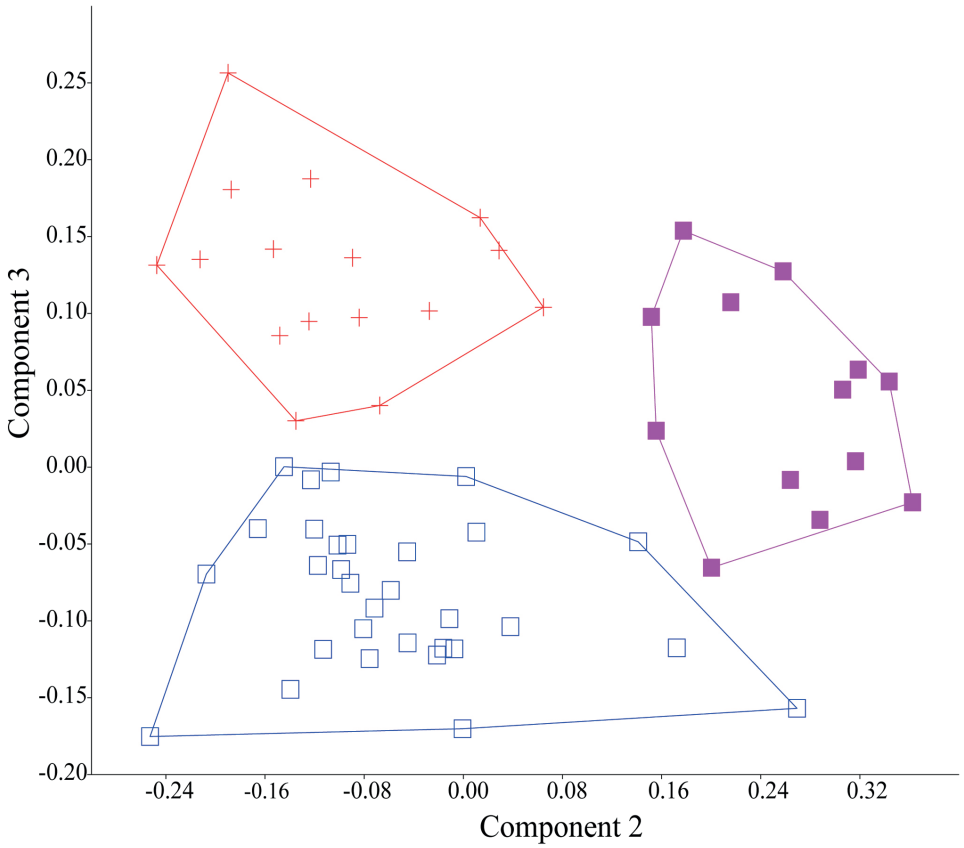

FIGURE 8 | Second and third principal components axes of combined samples of *Rhyacoglanis varii* (red cross, n = 16), *R. paranensis* (blue square; n = 31), and *R. rapppydanielae* (pink square; n = 13).

DNA barcode analysis. The Kimura 2-parameters genetic distance (K2P) between *Rhyacoglanis varii* and its congeners ranged from 1.9% (*R. paranensis*) to 3.4% (*R. annulatus*), with low intraspecific variation (Tab. 3). Based on COI gene sequences, species delimitation methods identified 7 MOTUs, corroborating *R. varii* as a new species. GMYC results indicated seven species with a confidence interval of 5 to 8 species; the maximum likelihood of the null model = 169.5058, the maximum likelihood of the GMYC model = 175.6366, and the threshold time = -0.0034. ABGD analysis resulted in 7 partitions where partition one (maximum previous distance p = 0.001) indicated 7 MOTUs. ASAP analysis retrieved nine partitions, with the lowest scoring partition (2.5) finding 7 MOTUs. The maximum likelihood solution of bPTP delimited 7 MOTUs and suggested a clear separation between the analyzed species. In the Bayesian inference analysis, *R. varii* was closely related to *R. paranensis*, and *R. annulatus* was the sister group of these two species. *Rhyacoglanis* sp. from the upper rio Araguaia basin (Fig. 9) was the basal species of the clade and was not closely related to *R. varii*. All *Rhyacoglanis* species clustered in a clade with high posterior probability support (Fig. 10), corroborating the monophyly of the genus. *Pseudopimelodus* and *Cruciglanis* were more closely related to each other than to *Rhyacoglanis*.

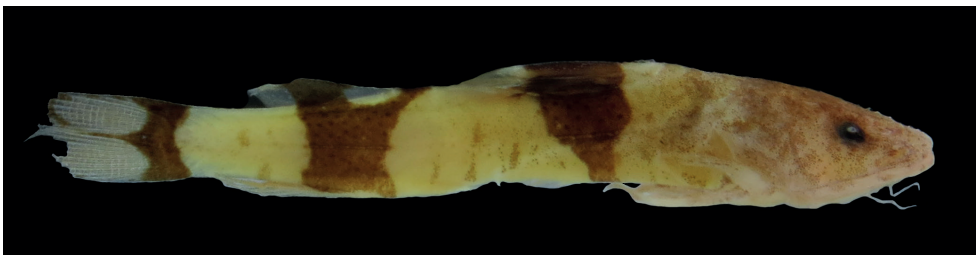

FIGURE 9 | Lateral view of sequenced *Rhyacoglanis* sp., LBP 1685, 21.6 mm SL, from Barra do Garças, state of Goiás, upper rio Araguaia basin.

FIGURE 10 | Pseudopimelodidae species delimitation with Bayesian GMYC analysis. The cluster of supported species is indicated in red, and the *Rhyacoglanis* cluster is highlighted in yellow ocher. The numbers on the nodes represent the posterior probability, and the branch length represents the time in My. Genbank accession number in parenthesis; * = specimens identified as *Pseudopimelodus mangurus* in Genbank.

TABLE 3 | Interspecific and intraspecific genetic distances are based on the mitochondrial gene cytochrome c oxidase I (COI). Values are shown as proportions. Intraspecific distances are in bold.

Species	1	2	3	4	5	6	7
1. *Rhyacoglanis varii*	**0.000**						
2. *Rhyacoglanis* sp. (Araguaia)	0.029	-					
3. *Rhyacoglanis paranensis*	0.019	0.041	**0.000**				
4. *Rhyacoglanis annulatus*	0.034	0.060	0.048	**0.003**			
5. *Cruciglanis pacifici*	0.138	0.130	0.149	0.152	**0.006**		
6. *Pseudopimelodus bufonius*	0.093	0.101	0.102	0.116	0.117	**0.003**	
7. *Pseudopimelodus mangurus*	0.107	0.109	0.109	0.118	0.109	0.027	**0.003**

Rhyacoglanis varii was recovered from different methods of species delimitation using molecular analysis. The results of those methods are presented as supplementary material: Fig. **S1**, Neighbor-joining tree; Fig. **S2**, Number of groups obtained with ABGD method; Fig. **S3**, Number of groups obtained with ASAP method; Tab. **S4**, GMYC method, and Fig. **S5**, Phylogeny of analyzed Pseudopimelodidae species obtained with bPTP method.

DISCUSSION

The new species was undoubtedly allocated to the genus *Rhyacoglanis* by sharing synapomorphies such as a pale spot on the cheek, a dark band across the upper and lower lobes of the posterior third of caudal-fin confluent with a dark bar on the caudal peduncle, and crest on the *cerebellum*'s parasagittal plane (Shibatta, Vari, 2017; Abrahão *et al*., 2018; Shibatta *et al*., 2021).

The caudal skeleton was essential to diagnose *Rhyacoglanis varii* from its cogener in the Tocantins basin, *R. rapppydanielae*. In *R. varii*, the caudal skeleton is composed of fused parhypural, hypurals 1 and 2, fused hypurals 3 and 4, and free hypural 5. In contrast, hypurals 3, 4, and 5 are fused in *R. rapppydanielae* of the lower rio Tocantins basin. The condition observed in *R. varii* and other congeners is considered plesiomorphic because it is present in *Pseudopimelodus mangurus* (Valenciennes, 1835) (Shibatta *et al*., 2021). On the other hand, the condition in *R. rapppydanielae* is autapomorphic.

The distribution of serrae along the anterior margin of the pectoral-fin spine distinguishes *R. varii* from *R. pulcher* and *R. seminiger*, two species in which serrae are restricted to the proximal portion of the spine. A distribution of serrae like *R. varii* is observed in *R. annulatus*, *R. paranensis*, *R. rapppydanielae*, and *R. seminiger*. In *R. varii*, the largest anterior serrae are about half the length of the largest posterior serrae, distinguishing it from *R. annulatus*, *R. rapppydanielae*, and *R. seminiger*, in which anterior and posterior serrae are the same size. Although only *R. paranensis* presents the distribution and dimensions of serrae like *R. varii*, barcoding, coloration, and morphometrics analysis distinguish the two species.

The post-cleithral process and caudal-fin shape distinguish two putative monophyletic groups of *Rhyacoglanis* species. *Rhyacoglanis varii* shares a long post-cleithral process and pointed caudal fin lobes with *R. annulatus*, *R. paranensis*, *R. pulcher*, and *R. seminiger*. Another group, formed by *R. epiblepsis* and *R. rapppydanielae*, has a shorter post-cleithral process and caudal fin with rounded lobes. The long post-cleithral process is present in other genera of Pseudopimelodidae, except in *Pseudopimelodus*. It evidences short post-cleithral process as an apomorphic condition. Therefore, the length of the post-cleithral process in *R. epiblepsis* and *R. rapppydanielae* seems to be a synapomorphy.

The species delimitation based on the K2P shows *R. varii* with a distance slightly lower than 2% from *R. paranensis*. The 2% value is the threshold that generally differentiates more than 99.2% of Neotropical fish species (Pereira *et al*., 2013), but lower distances have been used to delimit species by other authors (*e.g*., Ward *et al*., 2009; Pereira *et al*., 2013). As Pereira *et al*. (2013) argued, the 2% value may lead to an underestimation of the number of species. Therefore, other methods of analysis are essential for species delimitation.

The different species delimitation methods (GMYC, ABGD, ASAP, and bPTP analyses) supported *Rhyacoglanis varii* as a valid species, indicating it is phylogenetically closer to *R. paranensis* than to *R. annulatus*. These results are consistent with the biogeographic history of the upper rio Tocantins and upper rio Paraná basins. Aquino, Colli (2017) report the recent colonization of headwaters of the upper Tocantins by the fish assemblage of the upper Paraná and São Francisco basins. The baseline of the upper Tocantins basin is lower than that of the upper Paraná basin because of a descending structural gradient due to an active lift in the middle Tocantins-Araguaia basin. This event follows the Trans Brazilian Lineament (Saadi, 1993) that resulted in the Tocantins-Araguaia basin's tendency to capture watersheds of adjacent basins.

The differences in DNA barcodes between specimens from the upper rio Araguaia basin and the upper rio Tocantins basin were unexpected since the morphological characters (morphometrics and meristics) did not distinguish them. Added is the difficulty of identifying species as an individual sequenced from the upper rio Araguaia. Although the specimen is unequivocally *Rhyacoglanis*, the morphometry is imprecise due to its small size and deformation caused by dehydration in absolute ethanol and the removal of musculature from the left side of the body. Thus, all specimens from upper rio Araguaia were provisionally identified as *Rhyacoglanis* sp. and not included in the type series of *R. varii*.

Rhyacoglanis species inhabit the rapids of small to medium rivers. Therefore, the geographical distribution of *R. varii* can be concentrated in the upper regions of the rio Tocantins, where rapids are commonly formed by the escarpments of the Southern Plateau (or Planalto Meridional) of the Brazilian Shield. The differences between DNA barcodes associated with the upper Araguaia and upper Tocantins basins may represent a different history of headwater captures. The endemicity of fishes in upper rio Araguaia was pointed out by Lima, Moreira (2003), and Jarduli *et al*. (2014). The close association between *Rhyacoglanis* species and rapids makes them susceptible to stream modification caused by the dam. According to Chamon *et al*. (2022), hydroelectric power plants are the primary threat to the ichthyofauna in the Tocantins-Araguaia basin.

Comparative material examined. *Rhyacoglanis* sp. **Brazil**: All from rio Araguaia drainage. **Mato Grosso**. MZUSP 57481, 7, 23.0–66.2 mm SL, rio Areões, Nova Xavantina, 7 Jul 1969, J. Jim, V. C. Jesus & C. M. J. Spernega. LBP 1685, 1, 21.6 mm SL, rio das Garças, Barra do Garças, 15°54'18.1"S 52°19'24" W, 13 Dec 2002, C. Oliveira *et al*. MCP 40320, 1, 38.7 mm SL, rio das Mortes, Estação 1, Réguas, General Carneiro, 15°20'6.9"S 53°18'16.9"W, 11 Jan 2006, Equipe da CPA Ltda. MZUEL 07716, 6, 24.9–38.4 mm SL, tributary of rio Insula, Barra do Garças, 15°34'19.7"S 52°13'25.6"W, 1 Aug 2008, L. R. Jarduli, W. B. G. Ruiz & E. Santana. **Goiás**. MZUSP 105494, 1, 45.9 mm SL, tributary of rio do Peixe, under bridge of GO 164, km 84, Faina,15°20'51"S 50°24'30"W, 24 Jul 2005, Equipe CBE. MCP 41397, 1, 48.5 mm SL, rio Piranhas, próximo à foz do rio São Domingos, Piranhas, 16°33'6.0"S 51°49' 52.0"W, L. S. Rosa, F. L. Silveira & Z. Correa. 8 Nov 2005. MCP 41414, 2, 35.8–41.4 mm SL, rio Piranhas, próximo à foz do rio São Domingos, Piranhas, 16°33'6.0"S 51°49' 52.0"W, 23 Jul 2006, L. S. Rosa, F. L. Silveira & Z. Correa. MCP 41433, 1, 43.89–51.7 mm SL, rio Piranhas, próximo à foz do Córrego das Pedras, Piranhas, 16°32'3.0"S 51°49'58.0"W, 24 Jul 2006, L. S. Rosa, F. L. Silveira & Z. Correa.

ACKNOWLEDGMENTS

We thank Aléssio Datovo (MZUSP), Claudio de Oliveira (UNESP), and Roberto E. Reis (MCP) for loan of the specimens. Thanks to NAPI Taxonline – Conservação da Biodiversidade e Aplicações Tecnológicas (Fundação Araucária PI 02/2020) for MZUEL collection organization funding and for the LSS grant, and thanks to Conselho Nacional de Desenvolvimento Científico e Tecnológico (CNPq) for the research productivity grant to OAS (process #303685/2018-2).

REFERENCES

- **Abrahão VP, Pupo FM, Shibatta OA.** Comparative brain gross morphology of the Neotropical catfish family Pseudopimelodidae (Osteichthyes, Ostariophysi, Siluriformes), with phylogenetic implications. Zool J Linn Soc. 2018; 184(3):750–72. https://doi.org/10.1093/zoolinnean/zly011
- **Aquino PPU, Colli GR.** Headwater captures and the phylogenetic structure of freshwater fish assemblages: a case study in central Brazil. Jour Biogeog. 2017; 44(1):207–16. https://doi.org/10.1111/jbi.12870
- **Bouckaert R, Vaughan TG, Barido-Sottani J, Duchêne S, Fourment M, Gavryushkina A *et al*.** BEAST 2.5: An advanced software platform for Bayesian evolutionary analysis. PLoS Comput Biol. 2019; 15(4):e1006650. https://doi.org/10.1371/journal.pcbi.1006650
- **Chamon CC, Serra JP, Camelier P, Zanata AM, Fischberg I, Marinho MMF.** Building knowledge to save species: 20 years of ichthyofauna studies in the Tocantins-Araguaia River basin. Biota Neotrop. 2022; 22(2):e20211296. https://doi.org/10.1590/1676-0611-BN-2021-1296
- **Darriba D, Taboada GL, Doallo R, Posada D.** jModelTest 2: more models, new heuristics and parallel computing. Nat Methods. 2012; 9:772. https://doi.org/10.1038/nmeth.2109
- **Dingerkus G, Uhler LD.** Enzyme clearing alcian blue stained whole vertebrates for demonstration of cartilage. Stain Technol. 1977; 52(4):229–32. https://doi.org/10.3109/10520297709116780
- **Drummond AJ, Rambaut A.** BEAST: Bayesian evolutionary analysis by sampling trees. BMC Evol Biol. 2007; 7:214. https://doi.org/10.1186/1471-2148-7-214

- **Eigenmann CH.** The freshwater fishes of British Guiana, including a study of the ecological grouping of species, and the relation of the fauna of the plateau to that of the lowlands. Mem Carnegie Mus. 1912; 5(1):1–578.
- **Fujisawa T, Barraclough TG.** Delimiting species using single-locus data and the generalized mixed Yule coalescent approach: a revised method and evaluation on simulated data sets. Systematic Biol. 2013; 62(5):707–24. https://doi.org/10.1093/sysbio/syt033
- **Google Earth Pro.** Google Earth website. 2021. Available from: http://earth.google.com/
- **Hammer O, Harper DAT, Ryan PD.** PAST: Paleontological Statistics software package for education and data analysis. Palaeontol Electron. 2001; 4(1):1–09.
- **Hajibabaei M, deWaard JR, Ivanova NV, Ratnasingham S, Dooh RT, Kirk SL *et al*.** Critical factors for assembling a high volume of DNA barcodes. Phil Trans R Soc B. 2005; 360:1959–67. https://doi.org/10.1098/rstb.2005.1727
- **Heled J, Drummond AJ.** Bayesian inference of species trees from multilocus data. Mol Biol Evol. 2010; 27(3):570–80. https://doi.org/10.1093/molbev/msp274
- **International Union for Conservation of Nature (IUCN). Standards and petitions subcommittee.** Guidelines for using the IUCN Red List categories and criteria. Version 15.1 [Internet]. 2022. Available from: https://www.iucnredlist.org/resources/redlistguidelines
- **Jarduli LR, Claro-García A, Shibatta OA.** Ichthyofauna of the rio Araguaia basin, states of Mato Grosso and Goiás, Brazil. Check List. 2014; 10(3):483–515. https://doi.org/10.15560/10.3.483
- **Kimura M.** A simple method for estimating evolutionary rate of base substitutions through comparative studies of nucleotide sequences. Mol Evol. 1980; 16(2):111–20. https://doi.org/10.1007/bf01731581
- **Lima FCT, Moreira CR.** Three new species of *Hyphessobrycon* (Characiformes: Characidae) from the upper rio Araguaia basin in Brazil. Neotrop Ichthyol. 2003; 1(1):21–33. https://doi.org/10.1590/S1679-62252003000100003
- **Ortega-Lara A, Lehmann PA.** *Cruciglanis*, a new genus of Pseudopimelodid catfish (Ostariophysi: Siluriformes) with description of a new species from the Colombian Pacific coast. Neotrop Ichthyol. 2006; 4(2):147–56. https://doi.org/10.1590/S1679-62252006000200002
- **Pereira LHG, Hanner R, Foresti F, Oliveira C.** Can DNA barcoding accurately discriminate megadiverse Neotropical freshwater fish fauna? BMC Genetics. 2013; 14(20). https://doi.org/10.1186/1471-2156-14-20
- **Pons J, Barraclough TG, Gomez-Zurita J, Cardoso A, Duran DP, Hazell S *et al*.** Sequence-based species delimitation for the DNA taxonomy of undescribed insects. Syst Biol. 2006; 55(4):595–609. https://doi.org/10.1080/10635150600852011
- **Puillandre N, Lambert A, Brouillet S, Achaz GJME.** ABGD, Automatic Barcode Gap Discovery for primary species delimitation. Mol Ecol. 2012; 21(8):1864–77. https://doi.org/10.1111/j.1365-294x.2011.05239.x
- **Puillandre N, Brouillet S, Achaz G.** ASAP: assemble species by automatic partitioning. Mol Ecol Resour. 2021; 21(2):609–20. https://doi.org/10.1111/1755-0998.13281
- **QGIS Development Team.** QGIS 1.7.0 Geographic Information System. Open Source Geospatial Foundation Project; 2011. Available from: http://download.osgeo.org/qgis/doc/manual/<DOCUMENT>
- **Rambaut A.** FigTree. Tree figure drawing tool. 2009. Available from: http://tree.bio.ed.ac.uk/software/figtree/
- **Saadi A.** Neotectônica da Plataforma Brasileira: esboço e interpretação preliminares. Geonomos. 1993; 1(1):1–15. https://doi.org/10.18285/geonomos.v1i1e2.233
- **Shibatta OA.** New species of bumblebee catfish of the genus *Batrochoglanis* Gill, 1858 (Siluriformes: Pseudopimelodidae) from the Aripuanã River basin, Mato Grosso, Brazil. Zootaxa. 2019; 4674(2):243–63. https://doi.org/10.11646/zootaxa.4674.2.6

- **Shibatta OA, Jarduli LR, Abrahão VP, Souza-Shibatta L.** Phylogeny of the Neotropical Pacman catfish genus *Lophiosilurus* (Siluriformes: Pseudopimelodidae). Neotrop Ichthyol. 2021a; 19(4):e210040. https://doi.org/10.1590/1982-0224-2021-0040
- **Shibatta OA, Rocha MS, Oliveira RR.** New species of *Rhyacoglanis* (Siluriformes: Pseudopimelodidae) from rio Tocantins basin, northern Brazil. Neotrop Ichthyol. 2021b; 19(4):e210083. https://doi.org/10.1590/1982-0224-2021-0083
- **Shibatta OA, Vari RP.** A new genus of Neotropical rheophilic catfishes, with four new species (Teleostei: Siluriformes: Pseudopimelodidae). Neotrop Ichthyol. 2017; 15(2):e160132. http://dx.doi.org/10.1590/1982-0224-2016013
- **Silva GSC, Melo B, Roxo FF, Ochoa LE, Shibatta OA, Sabaj MH, Oliveira C.** Phylogenomics of the bumblebee catfishes (Siluriformes: Pseudopimelodidae) using ultraconserved elements. J Zool Syst Evol Res. 2021; 59(8):1662–72. https://doi.org/10.1111/jzs.12513
- **Tamura K, Stecher G, Peterson D, Filipski A, Kumar S.** MEGA6: molecular evolutionary genetics analysis version 6.0. Mol Biol Evol. 2013; 30(12):2725–29. https://doi.org/10.1093/molbev/mst197
- **Ward RD, Zemlak TS, Innes BH, Last PR, Hebert PDN.** DNA barcoding Australia's fish species. Phil Trans R Soc B. 2005; 360:1847–57. https://doi.org/10.1098/rstb.2005.1716
- **Winemiller KO, Mcintyre PB, Castello L, Fluet-Chouinard E, Giarrizzo T, Nam S *et al.*** Balancing hydropower and biodiversity in the Amazon, Congo, and Mekong. Science. 2016; 351(6269):128–29. https://doi.org/ 10.1126/science.aac7082
- **Zhang J, Kapli P, Pavlidis P, Stamatakis A.** A general species delimitation method with applications to phylogenetic placements. Bioinformatics 2013; 29(22):2869–76. https://doi.org/10.1093/bioinformatics/btt499

AUTHORS' CONTRIBUTION

Oscar Akio Shibatta: Conceptualization, Data curation, Formal analysis, Funding acquisition, Investigation, Methodology, Project administration, Resources, Software, Supervision, Validation, Visualization, Writing-original draft, Writing-review and editing.

Lenice Souza-Shibatta: Conceptualization, Data curation, Formal analysis, Funding acquisition, Investigation, Methodology, Project administration, Resources, Software, Supervision, Validation, Visualization, Writing-original draft, Writing-review and editing.

ETHICAL STATEMENT

Not applicable.

COMPETING INTERESTS

The author declares no competing interests.

HOW TO CITE THIS ARTICLE

- **Shibatta OA, Souza-Shibatta L.** New species of *Rhyacoglanis* (Siluriformes: Pseudopimelodidae) from the upper rio Tocantins basin. Neotrop Ichthyol. 2023; 21(1):e220075. https://doi.org/10.1590/1982-0224-2022-0075

Neotropical Ichthyology

OPEN ACCESS

Official Journal of the
Sociedade Brasileira de Ictiologia
SBI